Chemical synthesis and biological properties of pyridine epothilones*

KC Nicolaou [1], R Scarpelli [1], B Bollbuck [1], B Werschkun [1], MMA Pereira [1], M Wartmann [2], K-H Altmann [2], D Zaharevitz [3], R Gussio [3] and P Giannakakou [4]

Background: Numerous analogs of the antitumor agents epothilones A and B have been synthesized in search of better pharmacological profiles. Insights into the structure–activity relationships within the epothilone family are still needed and more potent and selective analogs of these compounds are in demand, both as biological tools and as chemotherapeutic agents, especially against drug-resistant tumors.

Results: A series of pyridine epothilone B analogs were designed, synthesized and screened. The synthesized compounds exhibited varying degrees of tubulin polymerization and cytotoxicity properties against a number of human cancer cell lines depending on the location of the nitrogen atom and the methyl substituent within the pyridine nucleus.

Conclusions: The biological screening results in this study established the importance of the nitrogen atom at the *ortho* position as well as the beneficial effect of a methyl substituent at the 4- or 5-position of the pyridine ring. Two pyridine epothilone B analogs (i.e. compounds **3** and **4**) possessing higher potencies against drug-resistant tumor cells than epothilone B, the most powerful of the naturally occurring epothilones, were identified.

[1]Department of Chemistry and The Skaggs Institute for Chemical Biology, The Scripps Research Institute, 10550 North Torrey Pines Road, La Jolla, CA 92037, USA and Department of Chemistry and Biochemistry, University of California, San Diego, 9500 Gilman Drive, La Jolla, CA 92093, USA
[2]Novartis Pharma AG, TA Oncology Research, CH-4002 Basel, Switzerland
[3]Target Structure-Based Drug Discovery Group, Information Technology Branch, Developmental Therapeutics Program, National Cancer Institute, NIH, Frederick, MD 21702, USA
[4]Medicine Branch, National Cancer Institute, NIH, Bethesda, MD 20892, USA

*This paper is dedicated to Professor José Barluenga on the occasion of his 60th birthday.

Correspondence: KC Nicolaou
E-mail: kcn@scripps.edu

Keywords: Antitumor activity; Chemical synthesis; Epothilones; Molecular modeling; Pyridine epothilones

Received: **28 February 2000**
Revisions requested: **4 April 2000**
Revisions received: **25 April 2000**
Accepted: **11 May 2000**

Published: **1 August 2000**

Chemistry & Biology 2000, **7**:593–599

1074-5521/00/$ – see front matter

PII: S1074-5521(00)00006-5

Introduction

The clinical success of paclitaxel (PTX) and docetaxel in the treatment of cancer has prompted a worldwide search for compounds with a similar mechanism of action but improved characteristics. The low aqueous solubility of PTX and the development of clinical drug resistance, mediated by both the overexpression of P-glycoprotein (P-pg) and the presence of β-tubulin mutations [1] are factors that hamper its applicability. The discovery [2] and recognition of the epothilones as potent tubulin polymerizing agents [3] propelled them into the forefront of chemical and biological research (for review see [4] and references therein). Hailed as superior antitumor agents to PTX, epothilones A (**1**) and B (**2**) (Figure 1) stimulated several total syntheses [5–16] and construction of numerous analogs with promising pharmacological profiles [4]. These studies [4] hinted at the importance of the nitrogen of the side chain as well as of the macrocyclic scaffold and its substituents for the biological activity of these molecules. In this communication we report the design, chemical synthesis and biological evaluation of a series of pyridine epothilone B analogs which establish the crucial role of these structural features for potent tubulin binding and cytotoxicity. Remarkably, two of these new analogs proved to be more potent against a variety of human cancer cell lines than epothilone B, the most active of the naturally occurring epothilones.

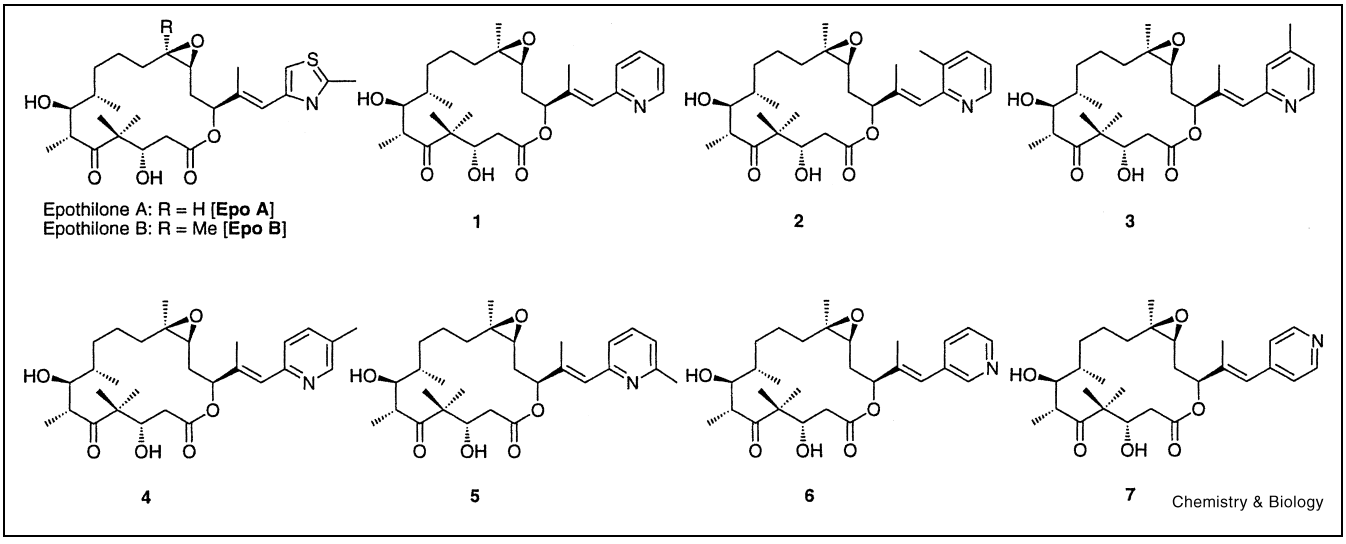

Figure 1. Molecular structures of Epo A and Epo B and designed pyridine epothilones B (**1**–**7**).

Results and discussion

Molecular design and chemical synthesis of pyridine epothilones

The molecular design of the reported epothilone analogs (**1**–**7**, Figure 1) was based on (a) the fact that epothilone B (Epo B) is considerably more potent than epothilone A (Epo A); and (b) the assumption that the nitrogen atom of the side chain needed to be at the strategic position that is found in the natural epothilones. The pyridine ring linked appropriately at the 2-position (analog **1**) was chosen as a substitute for the thiazole moiety. Molecular modeling [17] strongly suggested a role of this nitrogen as a hydrogen bond acceptor within the tubulin binding site, and to test this hypothesis the nitrogen atom was moved around the pyridine nucleus as in analogs **6** and **7**. To increase the lipophilicity of the molecule, a methyl group was introduced in the pyridine ring at all possible positions (analogs **2**–**5**).

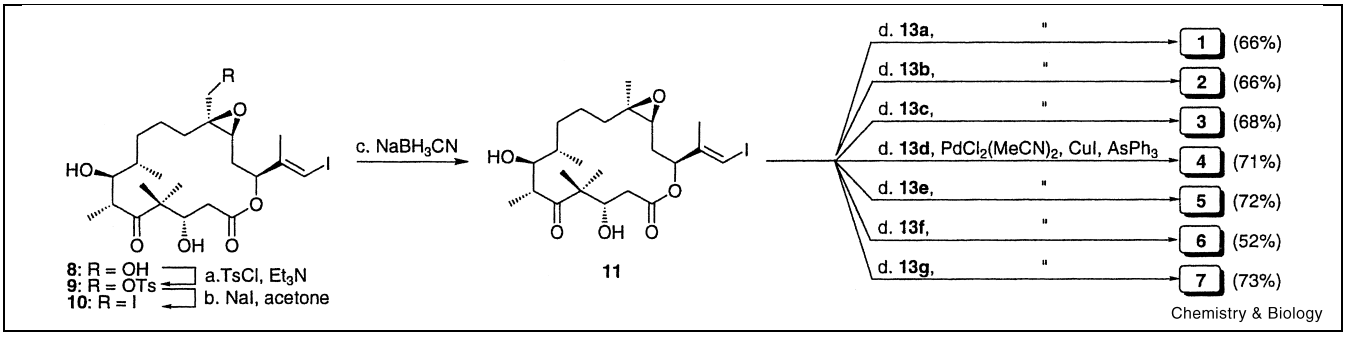

Scheme 1. Synthesis of designed pyridyl epothilones **1**–**7**. Reagents and conditions: (a) TsCl (1.5 equiv), Et_3N (3.0 equiv), 4-DMAP (1.0 equiv), CH_2Cl, 0–25°C, 1 h; (b) NaI (3.0 equiv), acetone, 25°C, 15 h, 75% (2 steps); (c) $NaBH_3CN$ (10.0 equiv), DMPU, 45°C, 40 h, 70%; (d) $PdCl_2(MeCN)_2$ (0.5 equiv), CuI (2.0 equiv), $AsPh_3$ (1.0 equiv), **13a**–**g** (2.5 equiv), DMF, 25°C, 1 h, 52–73%. Ts = *p*-toluenesulfonyl; 4-DMAP = 4-dimethylaminopyridine, DMPU = *N,N'*-dimethylpropyleneurea. **7**: $R_f = 0.71$ (silica gel, ethyl acetate); $[\alpha]_D^{22}$ −77.5 (*c* 1.3, $CHCl_3$); IR (thin film) ν_{max} 3441, 2930, 1735, 1682, 1600, 1460, 1376, 1260, 1148, 1054 cm^{-1}; ^1H NMR (600 MHz, $CDCl_3$) δ 8.35 (d, *J* = 4.8 Hz, 1H, Ar*H*), 7.08 (s, 1H, Ar*H*), 6.95 (d, *J* = 4.8 Hz, 1H, Ar*H*), 6.56 (s, 1H, C*H*=CCH$_3$), 5.38 (bs, 1H, CHO*H*), 5.35 (dd, *J* = 9.6, 1.8 Hz, 1H, CH_2COOCH), 4.38–4.32 (m, 1H, C*H*OH), 3.74–3.70 (m, 1H, C*H*OH), 3.29–3.24 (m, 1H, C(O)C*H*(CH$_3$)), 2.92 (bs, 1H, O*H*), 2.78 (dd, *J* = 8.8, 3.5 Hz, 1H, C*H*OCCH$_3$), 2.49 (dd, *J* = 13.2, 11.0 Hz, 1H, CH_2COOCH), 2.35 (s, 3H, ArCH_3), 2.31 (m, 1H), 2.25 (dd, *J* = 13.2, 2.6 Hz, 1H, CH_2COOCH), 2.20–2.14 (m, 1H, (CH$_3$)COCHCH_2CHO), 2.02 (s, 3H, CH=CCH_3), 1.88 (s, 3H, C(CH_3)OCHCH$_2$), 1.78–1.70 (m, 2H, CH_2C(CH$_3$)OCH), 1.64–1.56 (m, 1H), 1.54–1.40 (m, 3H), 1.32–1.28 (m, 1H), 1.26 (s, 3H, C(CH_3)$_2$), 1.13 (d, *J* = 6.6 Hz, 3H, CH(CH_3), 1.05 (s, 3H, C(CH_3)$_2$), 0.97 (d, *J* = 7.0 Hz, 3H, CH_3CHCHOH); ^{13}C NMR (150.9 MHz, $CDCl_3$) δ 220.7, 170.7, 155.2, 148.7, 147.8, 140.8, 125.1, 124.7, 122.6, 76.3, 71.5, 62.2, 61.7, 60.3, 53.9, 39.6, 36.1, 32.9, 32.3, 30.7, 22.5, 22.1, 21.7, 21.1, 20.9, 17.7, 16.8, 15.8, 14.1; MALDI HRMS (DHB) *m/z* 524.2983, M+Na$^+$ calcd. for $C_{29}H_{43}NO_6$ 524.2988.

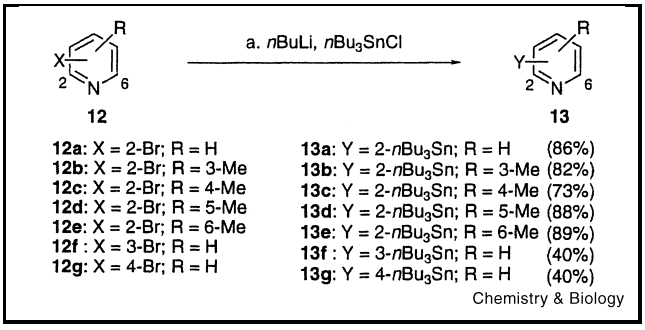

Scheme 2. Preparation of pyridine stannanes **13a–g**. Reagents and conditions: (a) *n*BuLi (1.1 equiv), THF, −78°C, 1 h, then add nBu$_3$SnCl (1.2 equiv), −78–25°C, 1 h, 40–89%.

The designed pyridine epothilones **1–7** were synthesized via a convergent approach as outlined in Scheme 1. The strategy [18,19] involved palladium-catalyzed coupling (Stille coupling) (for a recent review see [20]) of a common precursor, vinyl iodide **11** [19], with the appropriate pyridyl stannanes (**13a–g**, Scheme 2) providing directly the targeted compounds. Thus, the previously synthesized epothilone intermediate **8** [19] was selectively converted to tosylate **9** (TsCl, Et_3N), and thence to iodide **10** (NaI, 75% overall yield for two steps). The latter compound (**10**) was reduced with $NaBH_3CN$ to afford the desired vinyl iodide **11** in 70% yield. The required pyridyl stannanes **13a–g** were prepared from the corresponding, commercially available, bromopyridines **12a–g** (Scheme 2) via metal–halogen exchange (*n*BuLi) followed by quenching with nBu$_3$SnCl (40–89% yield, unoptimized). The Stille coupling of vinyl iodide **11** with stannanes **13a–g** proceeded smoothly in the presence of $PdCl_2(MeCN)_2$, CuI and $AsPh_3$ to afford epothilone analogs **1–7** in 52–73% yield (unoptimized) as shown in Scheme 1. The newly synthesized analogs were chromatographically purified (silica gel) and fully characterized by spectroscopic means (see legend of Scheme 1).

Molecular modeling

The pyridine analogs of epothilones were docked into the pharmacophore-refined tubulin model previously described [17]. Briefly, constrained molecular mechanics minimizations using the class II force field (CVFF91) were performed on acceptable pyridine conformers. The conformers that were considered acceptable had no van der Waals overlap with tubulin atoms above 0.25 Å, after rotations were performed in 3° increments, about the C15–C16 torsion. These rotatable bonds were explored until a full 360° rotation was completed. The C16–C17 and C17–C18 bonds were planar to the pyridine rings due to conjugation and support through PM3 semiempirical calculations. Pyridine conformers with nitrogens that were not solvent-exposed were rejected. Acceptable conformers were extended to include the *cis* and *trans* isomers of the 16-methyl substituent relative to the solvent-accessible surface of tubulin. These docking studies were performed for both wild-type (1A9) and mutant tubulin models (PTX10, A8, and B10) where deemed appropriate based on biological activity.

Biological evaluation

The synthesized epothilones were screened for their ability to induce in vitro tubulin polymerization using the filtration colorimetric assay (see Materials and methods Section) and Epo B was retested for comparison purposes. This analysis was then followed by cytotoxicity studies in a set of ovarian carcinoma cell lines, including a parental cell line (1A9) and four drug-resistant cell lines, namely two paclitaxel-resistant cell lines (1A9/PTX10 and 1A9/

Table 1
Biological properties of pyridine epothilones 1[a].

Compound	% TP[a]	Inhibition of ovarian carcinoma cell growth (IC_{50}) (nM)[b]				
		Parental	β-Tubulin mutant cells			
		1A9	PTX10 (β270)	PTX22 (β364)	A8 (β274)	B10 (β282)
Epo B	98	0.2	0.6 (3)[c]	0.2 (1)	5.4 (25)	5.2 (24)
1	79.5[d]	0.1	1 (10)	0.15 (1.5)	3 (30)	5 (50)
2	0	>300	>300	>300	>300	>300
3	90.3[d]	0.1	0.36 (3.6)	0.1 (1)	2.5 (25)	5 (50)
4	92	0.15	0.6 (4)	0.15 (1)	1.5 (10)	4 (27)
5	45	9	72 (8)	18 (2)	180 (20)	270 (30)
6	41.7[d]	1.7	35 (20)	8 (4.7)	23 (14)	10.5 (6)
7	34.5[d]	5.75	180 (31)	25 (4)	38 (6.6)	20 (3.4)

[a]The in vitro tubulin polymerization assay (% TP), the cytotoxicity assay and the origin and characteristics of the cell lines used are described in the Materials and methods Section.
[b]IC_{50} values in nM represent the average of one to three independent 96-h growth inhibition assays. IC_{50} is defined as the drug concentration that reduced cell protein by 50%.
[c]Values in parentheses are fold resistance factors, defined as the IC_{50} value obtained for the β-tubulin mutant divided by that obtained for the parental line.
[d]The percent tubulin polymerization values were calculated according to the method described in Table 2.

PTX22) [21] and two epothilone-resistant cell lines (1A9/A8 and 1A9/B10) [17] (see Table 1). These resistant cell lines harbor distinct acquired β-tubulin mutations which affect drug–tubulin interaction and result in impaired taxane- and epothilone-driven tubulin polymerization. In the atomic model of αβ-tubulin, these mutations are located near the taxane binding site [22]. The results of these biological investigations are summarized in Table 1 and reveal some important information for the structure–activity relationship of these compounds.

In general, there is good agreement between the in vitro tubulin polymerization potency and the cytotoxicity profile of all compounds tested. Interestingly, three compounds (**1**, **3** and **4**) were more potent in the cell growth inhibition assay against the parental 1A9 cells than Epo B, the most active of the naturally occurring epothilones. All three compounds retained a cross-resistance profile similar to Epo B against the four taxol- and Epo B-resistant cell lines revealing that substitution of the thiazole ring by a pyridine moiety (compound **1**) or with a 4- or 5-methylpyridine system (compounds **3** and **4**) is beneficial for biological activity (see below). Similarly to the thiazole side chain of Epo B, the presence of the nitrogen at the specific location shown is crucial for the interaction with tubulin as it, presumably, serves as a hydrogen bond acceptor. The fact that a similar cytotoxicity profile was obtained against the β-tubulin mutants potentially indicates that the conformation of these modified epothilones (**1**, **3** and **4**) does not change upon binding to tubulin so that the same groups that are important for Epo B binding remain instrumental for the interaction of these compounds with tubulin. In addition, compound **4** was more active than Epo B or compound **3** against the Epo-resistant 1A9/A8 cell line (fold resistance factors: 25 for Epo B and compound **3**, and 10 for compound **4**) that harbors the $\beta 274^{Thr \rightarrow Ile}$ mutation. This result suggests that the 5-methylpyridine system of compound **4** interacts more favorably with the hydrogen-bonded solvent network mediated by Ile at position β274. Compound **2** was inactive both in vitro (0% tubulin polymerization) and in cells ($IC_{50} > 300$ nM), i.e. placement of a methyl group at the 3-position of the pyridine ring results in total loss of activity. One possible explanation for this behavior is that the methyl group at the 3-position of the pyridine moiety forces the ring into an out-of-plane conformation with the neighboring double bond which is apparently unfavorable for binding to tubulin. Finally, compound **5** was much less potent than the parent Epo B, both in vitro and in cells, suggesting that the 6-methylpyridine substitution also leads to unfavorable changes in drug–tubulin interaction. The importance of the location of the nitrogen at the side chain was addressed by moving the nitrogen atom at two different positions on the pyridine ring. Molecular modeling predicted that the best position for the nitrogen atom would be the *ortho* position while relocation to the *meta* (compound **6**) or *para* (compound **7**) position would produce a significant loss of activity, with the rank order of activity being *ortho* > *meta* > *para*. This prediction was experimentally confirmed by both the in vitro tubulin polymerization and the cytotoxicity assay. As shown in Table 1, compound **6** is 17-fold less active against the 1A9 parental cells as compared to compound **1** which has the nitrogen at the *ortho* position (IC_{50} values, 1.7 and 0.1 nM, respectively) while compound **7** is 57.5-fold less active than compound **1** (IC_{50} values, 5.75 and 0.1 nM, respectively).

Table 2
Biological properties of pyridine epothilones. 2

Compound	% TP[b]	Cell growth inhibition of PTX-sensitive and PTX-resistant human cancer cell lines (IC_{50}) (nM)[a]									
		Epidermoid[c]		Lung[d]		Colon[e]		Prostate[f]		Breast[g]	
		KB-31	KB-8511	A549	NCIH460	HCT-15	HCT-116	DU-145	PC3-M	MCF-7	MCF-7/ADR
Epo B	85	0.18	0.18 (1)[h]	0.26	0.3	0.45	0.31	0.33	0.52	0.16	3.32 (20)
1	79.5	0.304	0.3 (1)	0.53	0.37	0.46	0.57	0.51	0.76	0.24	5.3 (22)
2	12	39.3	50.5 (1.28)	nd	nd	nd	nd	nd	nd	nd	nd
3	90.3	0.16	0.16 (1)	0.2	0.23	0.34	0.37	0.3	0.43	0.14	3.02 (21)
4	89.3	0.11	0.1 (1)	0.13	0.18	0.19	0.27	0.24	0.35	0.12	1.25 (10)
5	29.7	9.052	10.58 (1.17)	8.9	8.16	14.48	12.33	20.2	nd	7.07	nd
6	41.7	4.32	16.5 (3.8)	nd	nd	nd	nd	nd	nd	nd	nd
7	34.5	11.8	34.7 (2.94)	nd	nd	nd	nd	nd	nd	nd	nd
PTX	43.5	2.29	545.7 (238)	3.25	5.71	136.2	2.79	2.79	4.19	1.85	8984 (5005)

[a]The cytotoxicity assay and the calculation of IC_{50} values is described in the Materials and methods Section.
[b]The in vitro tubulin polymerization assay (% TP) is described in the Materials and methods Section.
[c]KB-31, PTX-sensitive, KB-8511, PTX-resistant due to P-gp overexpression, subline of KB-31.
[d]A549, NCIH460, PTX-sensitive.
[e]HCT-15, partially PTX-resistant due to P-gp overexpression, HCT-116, PTX-sensitive.
[f]DU-145, PC3-M, PTX-sensitive.
[g]MCF-7, PTX-sensitive, MCF-7/ADR, PTX-resistant due to P-gp overexpression, subline of the MCF-7 cell line.
[h]Values in parentheses are fold resistance factors defined as the IC_{50} value obtained for the drug-resistant subline divided by that obtained for the parental line.

The biological properties of the synthesized epothilones were also evaluated in a panel of human cancer cell lines of distinct origin as summarized in Table 2. In this table there are some cell lines resistant to PTX due to overexpression of P-gp. The cross-resistance profile of pyridine epothilones against the P-gp overexpressing cell lines suggests that they are far less favorable substrates for P-gp than PTX. For example PTX is 5000-fold less active against MCF-7/ADR cells as compared to parental MCF-7 cells, while Epo B and compounds **1**, **3**, and **4** are only 10–22-fold less active. Moreover, Epo B and compounds **1–7** retain almost full activity against the KB-8511 cells, in contrast to PTX which is 238-fold less active in this cell line compared to the parental KB-31 cells. In addition, the results of Table 2 show that compounds **3** and **4** are consistently more potent that the parent Epo B against the panel of the 10 human cancer cell lines tested, while compound **1** appears to be less potent in most cell lines. Similarly to the results presented in Table 1, compounds **6** and **7** are 14–39-fold less active than compound **1** against KB-31 cells, thus reinforcing the idea that the best placement for the nitrogen atom of the pyridine side chain is *ortho* to the attachment point of the ethenyl linker bridging the two ring domains of the epothilone structure.

The biological data for these pyridine epothilones are consistent with molecular docking experiments of these compounds within the common taxane-epothilone binding site according to our recently developed model of the interactions of Epo B with the energy-refined tubulin structure [17]. Figure 2 depicts compound **4** bound to its receptor site and surrounded by residues β-V21, β-F270 and β-T274. Noteworthy is the lipophilic extension of this compound provided by the 5-methyl substituent and which reaches closer to the lipophilic pocket formed by the β-V21 residue leading to enhanced interaction (higher potency). This binding mode provides the basis for the structure activity relationship of analogs **1–7** by our docking studies.

For example, according to the model of compound **1**, the unsubstituted pyridine is bulkier than the thiazole of Epo B. The model also indicates that this region of the taxane binding site is sterically restricted in such a way that the pyridine must occupy a conformation that is essentially

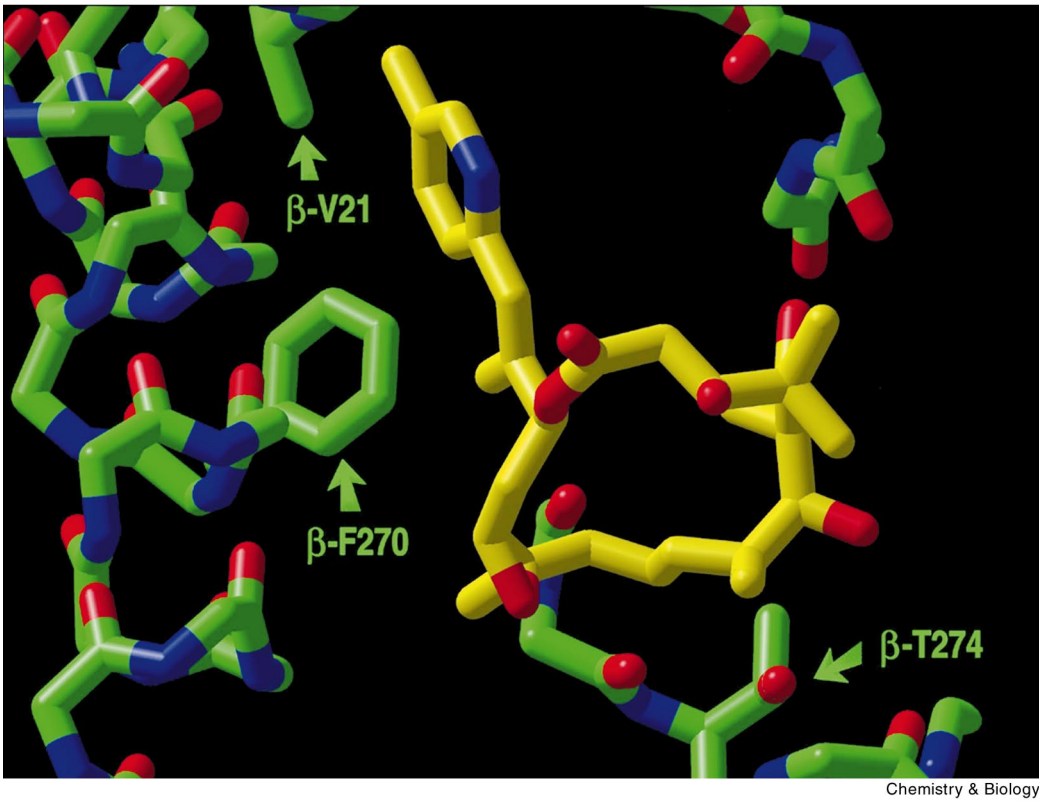

Figure 2. Stick model of compound **4** (carbon atoms in yellow) docked into an energy-refined model of tubulin. The backbone ribbon structure of tubulin is green. Arrows point at two residues that confer taxane and epothilone resistance (β270 and β274) and at one residue (β21) that makes a favorable hydrophobic contact with the 5-methyl group of the pyridine ring of compound **4**.

perpendicular to the solvent interface with tubulin. Such a conformation renders the pyridine nitrogen of **1** to be completely solvent-exposed which serves to facilitate hydrogen bonding with solvent. This modeling also indicates that the pyridine nitrogen that is *ortho* to the ring junction would be the only position on the pyridine where this hydrogen bond acceptor is completely solvent-exposed. The docking of compound **6** where the nitrogen of the pyridine is *meta* relative to the ring junction indicates that the nitrogen would be only partially accessible to the solvent. This prediction was confirmed with the marked decrease in activity of compound **6**. In addition, moving the pyridine nitrogen to the *para* position (as in compound **7**) further reduced the activity of this compound. This was predicted by docking studies of compound **7** due to the complete inaccessibility of the pyridine nitrogen of **7** to solvent.

Our modeling studies also indicate that the preferred conformation of the pyridine with the olefin group attached to carbon 18 is planar. This is supported by the docked conformation of compound **2**, where the methyl group at position 3 of the pyridine ring forces this ring out of plane with the olefin attached to 18. In this model, the entire side chain of **2** is parallel to the solvent-accessible surface of tubulin. This is a highly unfavorable binding mode, as the hydrophobic constituents of the pyridine ring are for the most part solvent-exposed. On the other hand, placing a methyl group at the 4-position of the pyridine ring (as in compound **3**) enables the pyridine–C16–C17 olefin system to form a planar conformation and make favorable hydrophobic contacts with the side chain of Ala231. However, similar to **1**, the extra bulk from the pyridine and methyl substituents imposes a steric restriction that shifts the entire molecule, including the macrolide ring system, approximately 1.0 Å away from the Epo B binding mode into the hydrogen-bonded network coordinated by Arg282 and Thr274. This may explain the increased sensitivity to both the epothilone-selected mutants A8 (β274) and B10 (β282) for compounds **1** and **3**. This result is consistent with the docking study of compound **4**. The placement of a methyl group onto pyridine, *para* to the ring junction (as in **4**), has the opposite effect of the 4-methyl substituent in **3**, or the absence of the methyl group in **1**. The most important effect of this change is that the 5-methyl group of compound **4** increases the overall length of the epothilone pyridine structure. As a consequence, **4** repositions itself away from the Phe270 which results in the 7-OH group of the macrolide being 1.28 Å away from Epo B's hydrogen-bonded solvent network, which is coordinated by Arg282 and Thr274. This model also indicates that **4** still retains its solvent-mediated hydrogen bond with Thr274. This may explain why **4** is more active against the A8 and B10 mutant cells compared to **1** and **3**.

Our modeling also explains the loss of activity of compound **5**. Docking shows that its 6-methyl group of the pyridine is exposed to solvent which creates a significantly less favorable binding mode, and decreases at the same time the solvent accessibility of this pyridine nitrogen. In concert with the repositioning of the pyridine nitrogen (as in compounds **6** and **7**), the previous finding underscores the notion that a six-membered ring requires a strong hydrogen bond acceptor in this solvent-exposed portion, when bound to tubulin.

In summary, we have identified two compounds (**3** and **4**) with superior biological activity over the parent Epo B, the most potent of the naturally occurring epothilones. Compound **4**, in particular, shows increased activity against the epothilone-resistant cell line A8 with a β274 tubulin mutation and is the most active of all the compounds tested against the P-gp overexpressing cell line MCF-7/ADR.

Significance

In conclusion, we have designed and synthesized a series of pyridine Epo B analogs, and established, through biological investigations and molecular modeling, the importance of the presence and location of the nitrogen for tubulin binding and cytotoxicity in these compounds. Most significantly, we have discovered that two of the newly synthesized pyridine epothilones exhibit more potent cytotoxic effects than Epo B against a wide variety of human cancer cells, including PTX- and Epo B-resistant cells. These findings are expected to aid further chemical biology studies and drug discovery efforts in the field of cancer chemotherapy.

Materials and methods

In vitro tubulin polymerization assay (Table 1)

Tubulin polymerization was determined by the filtration–colorimetric assay as previously described [3]. Briefly, 1 mg/ml of purified tubulin was incubated at 37°C for 30 min with 5 μM of each compound in MEM buffer [100 mM 2-(*N*-morpholino)ethanesulfonic acid, pH 6.75, 1 mM ethylene glycol bis(β-aminoethyl ether)-*N,N,N′,N′*-tetraacetic acid, 1 mM $MgCl_2$]. The mixture was then filtered to remove unpolymerized tubulin in a 96-well filtration plate (pore size, 0.22 μm) and the collected polymerized tubulin was stained with amido black solution and quantified by measuring absorbance of the dyed solution on a microplate reader. The percent polymerization was calculated relative to the absorbance produced by incubation with 0.5 M GTP+10% glycerol in MEM (presumed to cause 100% polymerization).

In vitro tubulin polymerization assay (Table 2)

Induction of tubulin polymerization was determined using a modified version of the microtubule protein centrifugation assay, as previously described [24]. MAP-associated porcine brain tubulin was incubated with 2 μM compound for 20 min. Percentage numbers indicate the relative degree of polymerization as compared to 25 μM Epo B, which under our experimental conditions caused $>95\%$ of the total tubulin to polymerize.

Cell culture and cytotoxicity assay (Table 1)

The epothilone-resistant cell lines 1A9/A8 and 1A9/B10 were isolated in a single step following exposure of the human ovarian carcinoma cell line A2780 (1A9) to lethal (IC_{99}) concentrations of either Epo A or B

(IC_{99} concentrations: 6 nM for Epo A and 0.5 nM for Epo B). After an initial expansion, the concentration of epothilones in the culture medium was gradually increased to 30 nM for Epo A and 5 nM for Epo B [17]. The isolation and characterization of the PTX-resistant cell lines 1A9/PTX10 and 1A9/PTX22 has been described elsewhere [21]. Cells were maintained in a 5% CO_2 humidified atmosphere at 37°C in RPMI medium 1640 (Gibco BRL) containing 10% fetal bovine serum, penicillin (100 U/ml) and streptomycin (100 μg/ml) (Gibco BRL). Prior to an experiment the 1A9/PTX10, 1A9/PTX22, 1A9/A8 and 1A9/B10 cells were cultured for at least 7–10 days in drug-free medium. Cytotoxicity assays were performed in 96-well plates using the sulforhodamine B assay as described previously [23] by seeding 500 cells/well and incubating with cytotoxic agents for 4 days.

Cytotoxicity assay (Table 2)

Antiproliferative assays were performed as previously described [25]. Briefly, cells were seeded at 1.5×10^3/well into 96-well microtiter plates and incubated overnight. Compounds were added in serial dilutions on day 1. Subsequently, the plates were incubated for two population doublings (3–5 days) and then fixed with 3.3% v/v glutaraldehyde, washed with water and stained with 0.05% methylene blue. After washing, the dye was eluted with 3% v/v HCl and the optical density measured at 665 nm with a SpectraMax 340 (Bucherer, Basel, Switzerland). IC_{50} values were determined by a computerized system (Softpro, Bucherer, Basel, Switzerland) using the formula $(OD_{treated} - OD_{start})/(OD_{control} - OD_{start}) \times 100$. IC_{50} is defined as the drug concentration which leads to 50% of cells per well as compared to control cultures (100%) at the end of the incubation period. The data represent the mean of three independent experiments.

Acknowledgements

The authors thank Drs. R. Reuter and M. Hattenberger from Novartis Pharma for the cell work as well as Drs. Gary Siuzdak and Dee H. Huang for mass spectrometry and NMR assistance, respectively. This work was financially supported by the National Institutes of Health (USA), The Skaggs Institute for Chemical Biology and Novartis Pharma, and fellowships from Università degli Studi di Roma 'La Sapienza' (to R.S.), Deutscher Akademischer Austauschdienst (DAAD) (to B.B.), Deutsche Forschungsgemeinschaft (to B.W.), and INVOTAN and FLAD (to M.M.A.P.).

References

1. Monzo, M., et al., & Martin, C. (1999). Paclitaxel resistance in non-small-cell lung cancer associated with beta-tubulin gene mutations. *J. Clin. Oncol.* **17**, 1786–1793.
2. Höfle, G., Bedorf, N., Steinmetz, H., Schomburg, D., Gerth, K. & Reichenbach, H. (1996). Antibiotics from gliding bacteria. 77. Epothilone A and B – novel 16-membered macrolides with cytotoxic activity isolation, crystal structure, and conformation in solution. *Angew. Chem. Int. Ed. Engl.* **35**, 1567–1569.
3. Bollag, D.M., et al., & Woods, C.M. (1995). Epothilones, a new class of microtubule-stabilizing agents with a taxol-like mechanism of action. *Cancer Res.* **55**, 2325–2333.
4. Nicolaou, K.C., Roschangar, F. & Vourloumis, D. (1998). Chemical biology of epothilones. *Angew. Chem. Int. Ed.* **37**, 2014–2045.
5. Balog, A., et al., & Danishefsky, S.J. (1996). Total synthesis of (−)-epothilone A. *Angew. Chem. Int. Ed. Engl.* **35**, 2801–2803.
6. Su, D.-S., et al., & Horwitz, S.B. (1997). Total synthesis of (−)-epothilone B: an extension of the Suzuki coupling method and insights into structure–activity relationships of the epothilones. *Angew. Chem. Int. Ed. Engl.* **36**, 757–759.
7. Meng, D., et al., & Danishefsky, S.J. (1997). Total syntheses of epothilones A and B. *J. Am. Chem. Soc.* **119**, 10073–10092.
8. Yang, Z., He, Y., Vourloumis, D., Vallberg, H. & Nicolaou, K.C. (1997). Total synthesis of epothilone A: the olefin metathesis approach. *Angew. Chem. Int. Ed. Engl.* **36**, 166–168.
9. Nicolaou, K.C., Sarabia, F., Ninkovic, S. & Yang, Z. (1997). Total synthesis of epothilone A: the macrolactonization approach. *Angew. Chem. Int. Ed. Engl.* **36**, 525–527.
10. Nicolaou, K.C., et al., & Hamel, E. (1997). Synthesis of epothilones A and B in solid and solution phase. *Nature* **387**, 268–272.
11. Schinzer, D., Limberg, A., Bauer, A., Böhm, O.M. & Cordes, M. (1997). Total synthesis of (−)-epothilone A. *Angew. Chem. Int. Ed. Engl.* **36**, 523–524.
12. May, S. & Grieco, P.A. (1998). Total synthesis of (−)-epothilone B. *Chem. Commun.* 1597–1598.
13. White, J.D., Sundermann, K.F. & Carter, R.G. (1999). Improved synthesis of epothilone B employing alkylation of an alkyne for assembly of subunits. *Org. Lett.* **1**, 1431–1434.
14. Sinha, S.C., Sun, J., Miller, G., Barbas III, C.F. & Lerner, R.A. (1999). Sets of aldolase antibodies with antipodal reactivities. Formal synthesis of epothilone E by large-scale antibody-catalyzed resolution of thiazole aldol. *Org. Lett.* **1**, 1623–1626.
15. Sawada, D. & Shibasaki, M. (2000). Enantioselective total synthesis of epothilone A using multifunctional asymmetric catalyses. *Angew. Chem. Int. Ed.* **39**, 209–213.
16. Martin, H.J., Drescher, M. & Mulzer, J. (2000). How stable are epoxides? A novel synthesis of epothilone B. *Angew. Chem. Int. Ed.* **39**, 581–583.
17. Giannakakou, P., et al., & Fojo, T. (2000). A common pharmacophore for epothilones and taxanes: molecular basis for drug resistance-conferred by tubulin mutations in human cancer cells. *Proc. Natl. Acad. Sci. USA* **97**, 2904–2909.
18. Nicolaou, K.C., He, Y., Roschangar, F., King, N.P., Vourloumis, D. & Li, T. (1998). Total synthesis of epothilone E and analogues with modified side chains through the Stille coupling reaction. *Angew. Chem. Int. Ed. Engl.* **37**, 84–87.
19. Nicolaou, K.C., et al., & Hepworth, D. (1999). Total synthesis of epothilone E and related side chain modified analogs via a Stille coupling based strategy. *Bioorg. Med. Chem.* **7**, 665–697.
20. Farina, V., Krishnamurthy, V. & Scott, J.W. (1997). The Stille reaction. In *Organic Reactions*. (Paquette, L., ed.), Vol. 50, pp. 1–41, John Wiley & Sons, New York.
21. Giannakakou, P., et al., & Poruchynsky, M.S. (1997). Paclitaxel-resistant human ovarian cancer cells have mutant β-tubulins that exhibit impaired paclitaxel-driven polymerization. *J. Biol. Chem.* **272**, 17118–17125.
22. Nogales, E., Wolf, S.G. & Downing, K.H. (1998). Structure of the αβ tubulin dimer by electron crystallography. *Nature* **391**, 191–203.
23. Skehan, P., et al., & Boyd, M.R. (1990). New colorimetric cytotoxicity assay for anticancer-drug screening. *J. Natl. Cancer Inst.* **82**, 1107–1112.
24. Lin, C.M., Jiang, Y.Q., Chaudhary, A.G., Rimoldi, J.M., Kingston, D.G.I. & Hamel, E. (1996). A convenient tubulin-based quantitative assay for paclitaxel (Taxol) derivatives more effective in inducing assembly than parent compound. *Cancer Chem. Pharm.* **38**, 136–140.
25. Meyer, T., et al., & Matter, A. (1989). A derivative of staurosporine (CGP 41251) shows selectivity for protein kinase C inhibition and in vitro anti-proliferative as well as in vivo anti-tumor activity. *Int. J. Cancer* **43**, 851–856.